Loxodromic Antenna Arrays Based on Archimedean Spiral

Original Scientific Paper

Slavko Rupčić

Josip Juraj Strossmayer University of Osijek,
Faculty of Electrical Engineering, Department of Communications
KnezaTrpimira 2b, Osijek, Croatia
slavko.rupcic@etfos.hr

Vanja Mandrić Radivojević

Josip Juraj Strossmayer University of Osijek,
Faculty of Electrical Engineering, Department of Communications
KnezaTrpimira 2b, Osijek, Croatia
vanja.mandric@etfos.hr

Krešimir Grgić

Josip Juraj Strossmayer University of Osijek,
Faculty of Electrical Engineering, Department of Communications
KnezaTrpimira 2b, Osijek, Croatia
kresimir.grgic@etfos.hr

Abstract – *A loxodromic antenna array is a spiral array on the spherical surface. Distribution of elementary antennas on the spherical surface was made by following loxodromic curves. This type of antenna array offers a wide range of opportunities in the variation of their radiation patterns through antenna distribution and phase control. The paper studies different loxodromic antenna arrays based on the influence of an Archimedean spiral configuration pattern on the radiation pattern of a spherical antenna array. Analysis was made using a developed moment method program with a spectral-domain approach.*

Keywords – *Archimedean spiral, conformal antennas, loxodromic configuration, method of moment, radiation pattern, spherical array*

1. INTRODUCTION

As several papers before [1-5], this paper deals with circular microstrip elementary antennas mounted on a spherical surface constituting one of many possible types of conformal antenna arrays. All conformal antennas have a few good common characteristics: the ability to mold to curved shaped surfaces, the ability to produce the desired radiation pattern, and finally, the capability of providing electronic scan coverage over the whole sphere. Such antennas could satisfy requirements for many applications.

Earlier research [1-5] showed that a spiral type of antenna array gives very good results in the radiation pattern context. This means it is possible to achieve a narrow main lobe and low-level side lobes. Far field calculation is made in Section 2 of this paper. A radiation pattern was calculated by using the method of moment and the spectral-domain approach.

Section 3 deals with spiral distributions of antenna elements on the spherical surface.

Section 4 analyzes and compares different types of Archimedean spiral distributions of elementary antennas mounted on spherical surfaces.

2. FAR FIELD CALCULATION

Elementary antennas are mounted on a grounded conducting spherical shaped plane. Because of the spherical radiating structure, radiation problems will be solved using the spherical coordinate system. A spherical array of spiral distribution of microstrip antennas is analyzed using the method of moment in a spectral-domain. The spectral-domain technique transforms a three-dimensional problem into a spectrum of one-dimensional problem, which is easier to solve [6], [7]. This spectrum is obtained by applying the vector-Legendre transformation to the real current density at the circular microstrip antennas. An electrical field radiated by the current shell on the spherical surface in homogeneous media is:

$$E(r,\theta,\phi) = \sum_{m=\infty}^{\infty} \sum_{n=|m|}^{\infty} \overline{\overline{L}}(n,m,\theta)\overline{\overline{\widetilde{G}}}(n,m,r \mid r_s)\widetilde{C}(r,n,m)e^{jm\phi} \quad (1)$$

where m and n are the variables in the spectral domain, $\overline{\overline{G}}(n,m,r\mid r_s)$ is a spectral-domain dyadic Green's function for a grounded spherical surface, $\overline{\overline{L}}(n,m,\theta)$ is the kernel of the vector-Legendre transformation and $\widetilde{C}(r,n,m)$ is a spectral domain current placed at each antenna element.

G1DMULT is an algorithm used for calculating the spectral-domain Green's function of a multilayer spherical structure [7].

The radiation pattern of the array is obtained as a superposition of fields excited by each antenna:

$$\mathrm{E}(\theta,\phi) = \sum_{n,m} E_{\alpha_n \beta_m}(\theta,\phi) \qquad (2)$$

3. SPIRAL DISTRIBUTION OF ANTENNA ELEMENTS ON THE SPHERE

Antennas could be placed by several rules (nonuniform) on a spherical surface [1], [5]. One of them is spiral, and that type of configuration has the ability to satisfy requirements on communications demands like achieving optimum signal reception in any spherical space direction without altering the radiated pattern. This is antenna configuration which appears for a large N, where N is the number of elements in a radiating system [1].
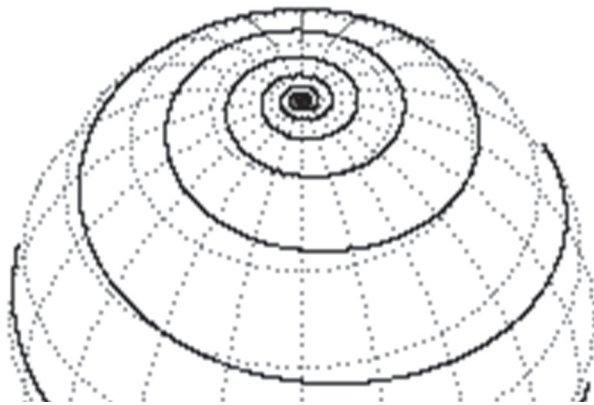

Fig. 1. Loxodromic curves which spiral towards the north pole.

Some investigations on spiral type of spherical antennas are made in [1], [4], [5], etc., so we decided to make a step further in evaluating and improving radiating pattern characteristics. This paper analyzes and compares three different types of spiral configurations, i.e., the Archimedean spiral based on one, two and three arms. Their optimization will be left for future research.

A spiral curve projected on a 3D sphere is called a loxodromic curve (Figure 2). This kind of mathematical term is very important in this context because of its great contribution to antenna theory design (by the ability to mold to curved shaped surfaces, it is possible to produce the desired radiation pattern, provide electronic scan coverage over the whole sphere, and above all, requirements can be satisfied for many applications in radio communications).

It is well known that constellations with antennas grouped around angles of maximum radiation have a narrow main lobe and low-level side lobes. Because of the need to achieve the desirable radiation pattern, we decided to analyze those three types of spiral configuration.
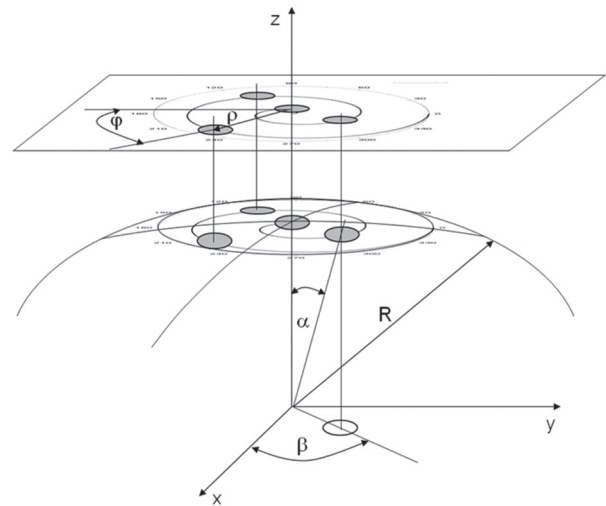

Fig. 2. Loxodromic Archimedean spiral antenna array.

3.1. ARCHIMEDEAN SPIRAL DISTRIBUTION

Generally, a spiral curve is given by the equation:

$$\rho = a\varphi^n, \qquad (3)$$

where *a* is a real number and it is assumed that a > 0.

Figure 1. shows a general shape of a spiral curve projected on the sphere -a so-called loxodromic curve. A special case when n = 1 is an Archimedean spiral [8]. The Archimedean spiral is the locus of points corresponding to the locations over time of a point moving away from a fixed point with a constant speed along a line which rotates with constant angular velocity. In polar coordinates, a one-arm Archimedean spiral can be described by the equation:

$$\rho = a\varphi. \qquad (4)$$

A two-arm Archimedean spiral can be described by:

$$\rho_1 = a\varphi, \qquad (5)$$
$$\rho_2 = a(\varphi - 180°), \qquad (6)$$

while a three-arm Archimedean spiral can be described by the following:

$$\rho_1 = a\varphi, \qquad (7)$$
$$\rho_2 = a(\varphi - 120°), \qquad (8)$$
$$\rho_3 = a(\varphi - 240°). \qquad (9)$$

Based on the previous mathematical presentations, the Archimedean spiral is displayed in Figures 3, 4 and 5, respectively.

Circular microstrip antennas are placed on the grounded sphere following the above rules. If those equations are taken into consideration, antenna arrays could be constituted with 19 microstrip antennas (a one-arm Archimedean spiral path), 38 microstrip antennas (a two-arm Archimedean spiral path) and 57microstrip antennas (a three-arm Archimedean spiral path). For the second and third case, antenna origins are separated into 180° and 120°, respectively.
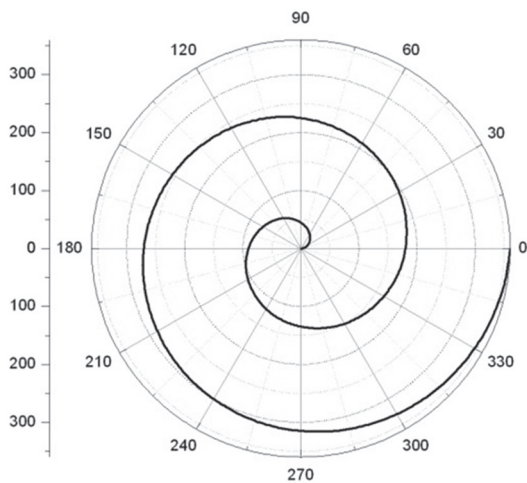
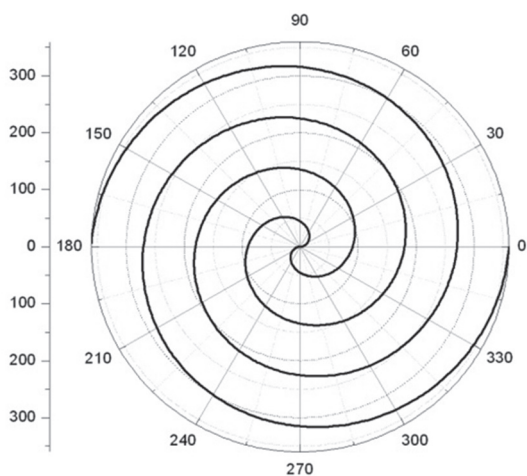**Fig. 3.** A one-arm Archimedean spiral ($\rho = a\varphi$).

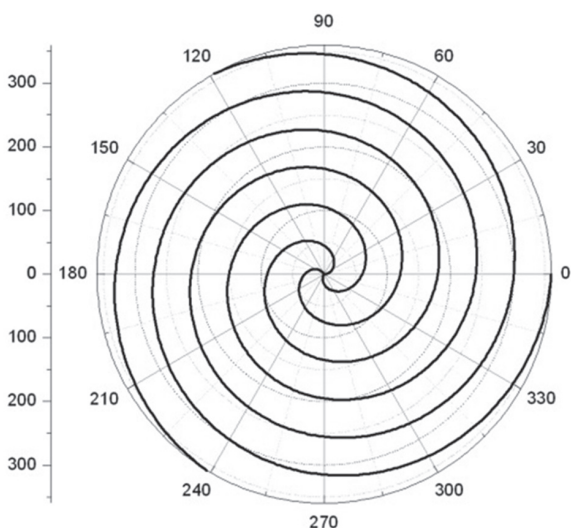**Fig. 4.** A two-arm Archimedean spiral ($\rho_1 = a\varphi$ and $\rho_2 = a(\varphi-180°)$).

Fig. 5. A three-arm Archimedean spiral ($\rho_1 = a\rho$, $\rho_2 = a(\varphi-120°)$ and $\rho_3 = a(\varphi-240°)$).

Circular microstrip antennas are placed on the grounded sphere following the above rules. If those equations are taken into consideration, antenna arrays could be constituted with 19 microstrip antennas

(a one-arm Archimedean spiral path), 38 microstrip antennas (a two-arm Archimedean spiral path) and 57microstrip antennas (a three-arm Archimedean spiral path). For the second and third case, antenna origins are separated into 180° and 120°, respectively.

4. RESULTS

The goal of this paper is to investigate the influence of different spiral configurations of antennas on the radiation pattern of spherical antenna arrays. Figures 7, 9, 11, 12, 13 and 14 present normalized values of electric field amplitudes for one, two and three arms of Archimedean spiral distributions of elementary antennas mounted on spherical surfaces. Normalized radiation patterns were calculated at the frequency f = 1.70 GHz for the E and the H plane, respectively. The radius of the spherical surface is r=5λ, and the distance between antenna elements was limited to d ≥λ/2 (that distance is very important in coupling rules). d =λ/2 is the minimal distance between the central antenna ("north pole antenna") and the first (nearest) antenna of the spiral array. This distance between neighboring antennas for each considered geometry is enough to ensure low mutual coupling.

The radiation cone angle is 40 degrees. Patch antennas are excited by a coaxial feed (probe) and linearly polarized (parallel to the prime meridian plane).

A radiation pattern could be changed and improved by alternating a few parameters: a spiral constant a for every distribution type and, of course, antenna density.

4.1. ONE-ARM ARCHIMEDEAN SPIRAL DISTRIBUTION

It can be seen from distribution diagrams (Figures 6, 8 and 10) that spiral distribution in all analyzed types of arrays has "shifts". The reason for these shifts is the minimal distance between antenna elements, i.e., d ≥λ/2.The following figures also show radiation patterns for different situations - in (4), constant a is a variable. Radiation patterns are given separately in both orthogonal planes, E and H.
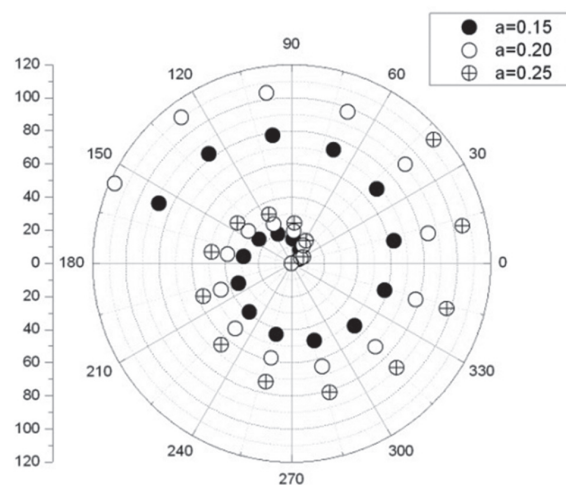

Fig. 6. One-arm Archimedean spiral distribution of a spherical antenna array.
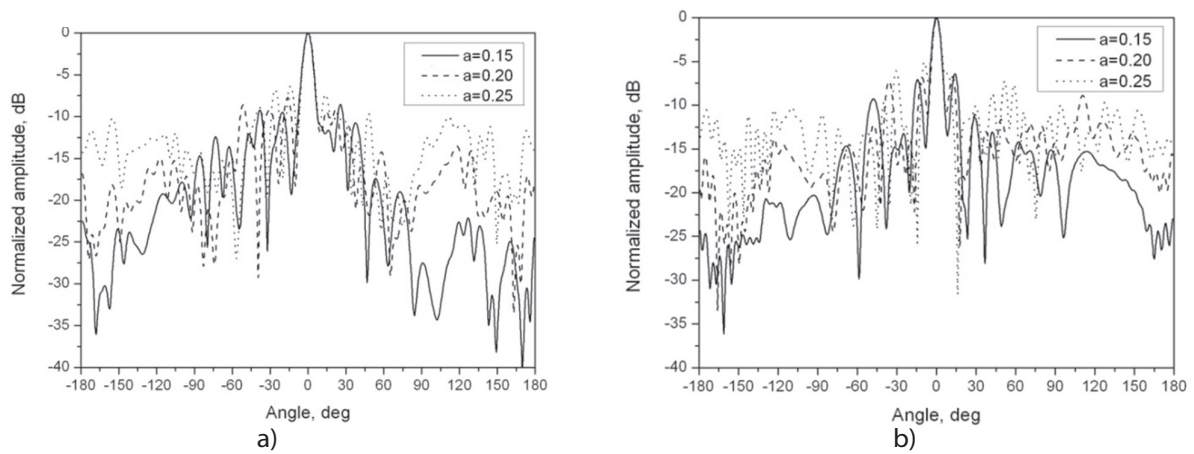
a)

b)

Fig. 7. Normalized calculated radiation pattern of one-arm Archimedean spiral distribution in a) E and b) H planes with different constant values.

When we look at these two diagrams (Figures 7a) and 7b)), it is obvious that in the E-plane, the beam width of the electrical field (the main lobe) at -3 dB does not change at all. The constant value of BW_{-3dB} is 7.88 degree. A similar conclusion applies to the H-plane, where BW_{-3dB} is about 6.80 deg. The situation with the side lobe level (SLL) is different. We can conclude that the SLL changes. This means that the SLL increases with an increase in the coefficient value from -8.53 dB to -6.34 dB for the E-plane, and from -6.43 dB to -5.05 dB in the H-plane.

4.2. TWO-ARM ARCHIMEDEAN SPIRAL DISTRIBUTION

As done and shown in the previous example, Figures 8 and 9 lead to a very similar conclusion. Different values of the constant significantly affect radiation patterns in both planes, as does the number of antennas on the sphere.

Table 1.

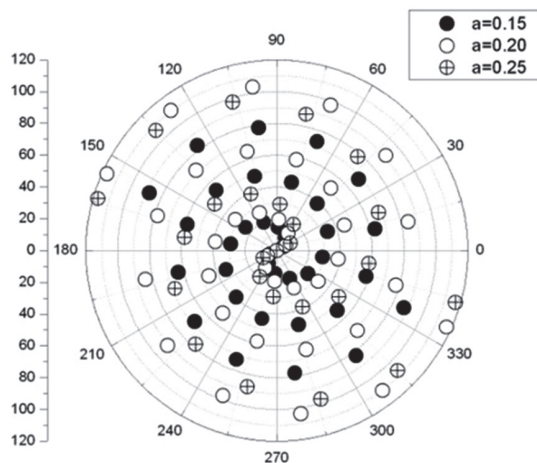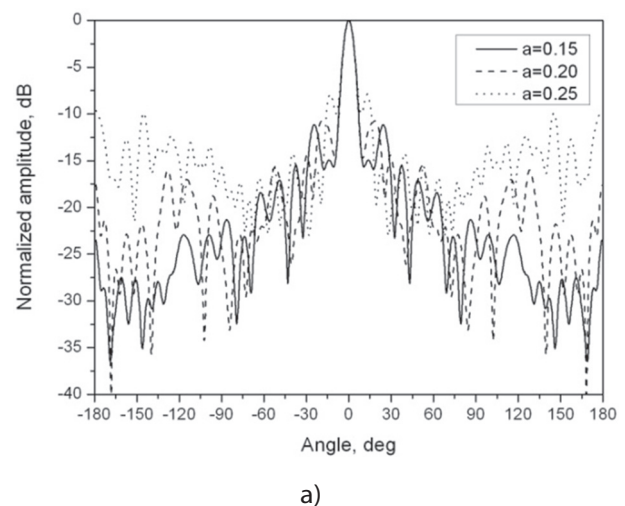|		One arm		Two arms		Three arms	
		BW_{-3dB}, deg	SLL, dB	BW_{-3dB}, deg	SLL, dB	BW_{-3dB}, deg	SLL, dB
E-plane	$a = 0.15$	7.88	-8.53	7.52	-11.15	7.52	-13.77
	$a = 0.20$	7.88	-7.71	7.52	-10.73	7.52	-12.82
	$a = 0.25$	7.88	-6.34	7.52	-7.87	7.52	-9.06
H-plane	$a = 0.15$	6.80	-6.43	6.80	-12.85	6.80	-12.09
	$a = 0.20$	6.44	-6.76	6.08	-9.93	6.08	-11.03
	$a = 0.25$	6.80	-5.05	6.08	-9.21	6.44	-8.61

Fig. 8. Two-arm Archimedean spiral distribution of a spherical antenna array.
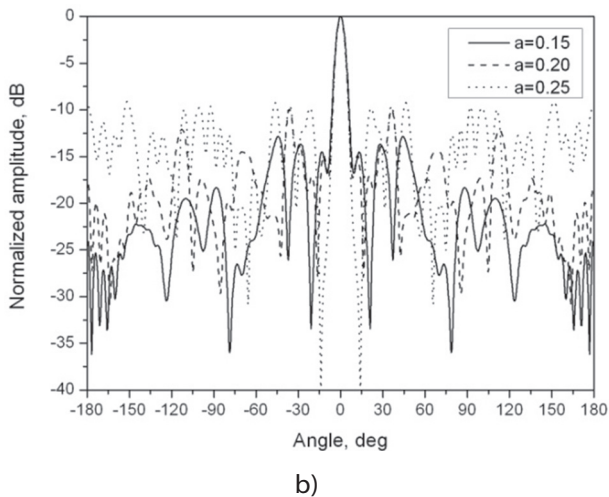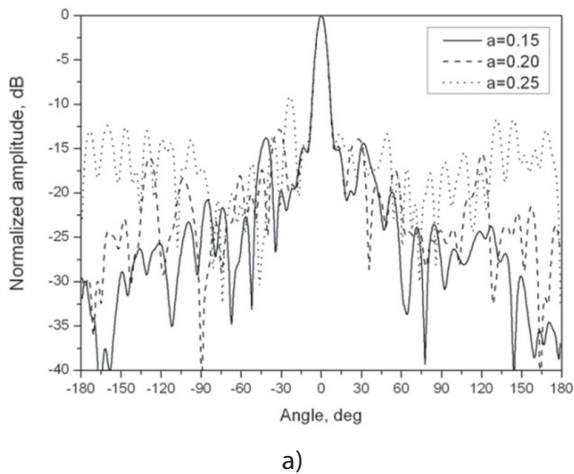

a)

b)

Fig. 9. Normalized calculated radiation pattern of two-arm Archimedean spiral distribution in a) E and b) H planes with different constant values.

Figures 9a) and 9b) show the situation that is the same as the situation in Figure 7. The main lobe width at -3 dB is 7.52 deg for each value of coefficient a in the E-plane. In the H-plane, BW_{-3dB} are 6.80 deg and 6.08 deg. The SLL changes with an increase in the coefficient a from -11.15 dB to -7.87 dB for the E-plane, and from -12.85 dB to -9.21 dB in the H-plane. All results are displayed in Table 1.

4.3. THREE- ARM ARCHIMEDEAN SPIRAL DISTRIBUTION

Three-arm Archimedean spiral distribution of antennas is the distribution with a large number of antennas in one array (Figure 10).
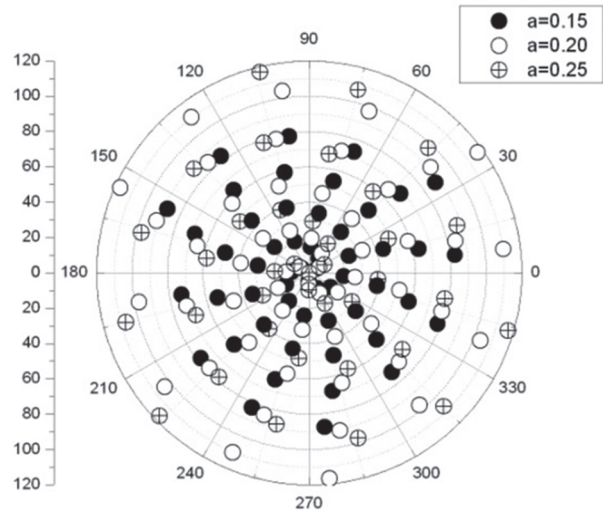

Fig. 10. Three-arm Archimedean spiral distribution of a spherical antenna array.
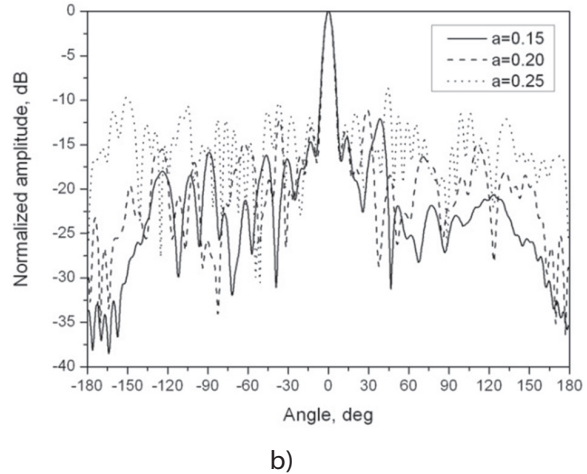

a)

b)

Fig. 11. Normalized calculated radiation pattern of three-arm Archimedean spiral distribution in a) E and b) H planes with different constant values.

It can be seen that variation of the constant a has a significant influence on the radiation pattern in terms of side lobe levels. A decrease in the parameter improves as a consequence radiation pattern characteristics. Side lobe levels could be decreased for about 4 dB for all cases (the E-plane and the H-plane, respectively - Table 1).

4.4. COMPARISON OF THREEARCHIMEDEAN SPIRAL DISTRIBUTIONS

A) The E and the H plane (phi=0⁰ and phi=90⁰, respectively)

As stated before, an increase in the number of antennas, or arms in this context, could also improve pattern characteristics. Changing constant a from 0.15 to 0.25

does not have a significant influence on the main lobe width at E = -3 dB. Figures 12, 13 and 14 confirm all these statements.

An increase in the number of antennas has improved the radiation pattern consequently (Figures 12, 13 and 14). If a = 0.15, the SLL decreases from -8.54 dB (a one-arm Archimedean spiral) to -13.78 dB (a three-arm Archimedean spiral) in the E-plane. The SLL decreases from -4.97 dB (a one-arm Archimedean spiral) to -12.11 dB (a three-arm Archimedean spiral) in the H-plane.

The same conclusion can be drawn for the third case when a = 0.25. The SLL decreases from -6.32 dB (a one-arm Archimedean spiral) to -9.04 dB (a three-arm Archi-

medean spiral) in the E-plane, and from -5.03 dB (a one-arm Archimedean spiral) to -8.59 dB (a three-arm Archimedean spiral) in the H-plane. The beam width at E = -3 dB does not change much in any situation (Table 1).
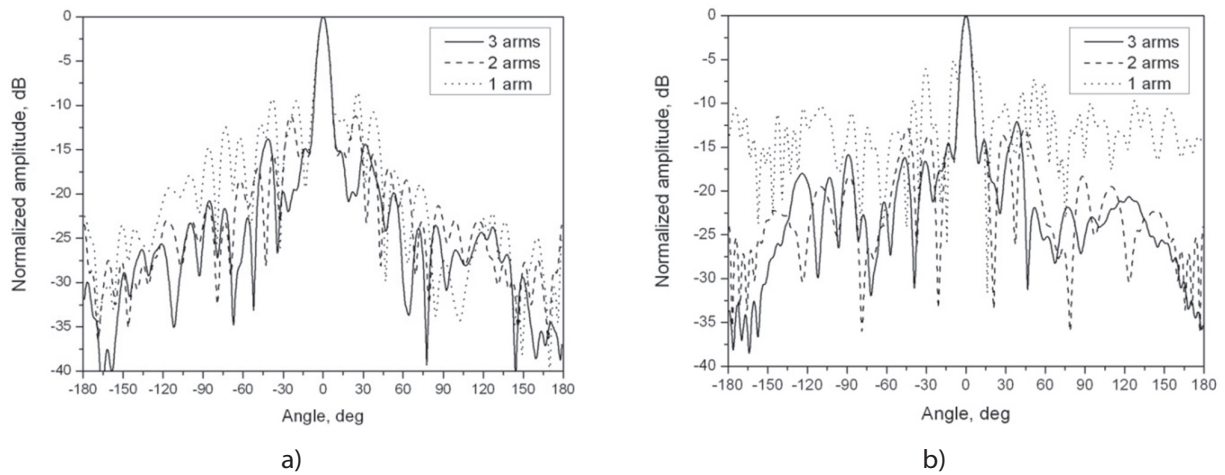

Fig. 12. Normalized radiation pattern for a different number of antennas if a = 0.15
a) the E plane and b) the H plane.

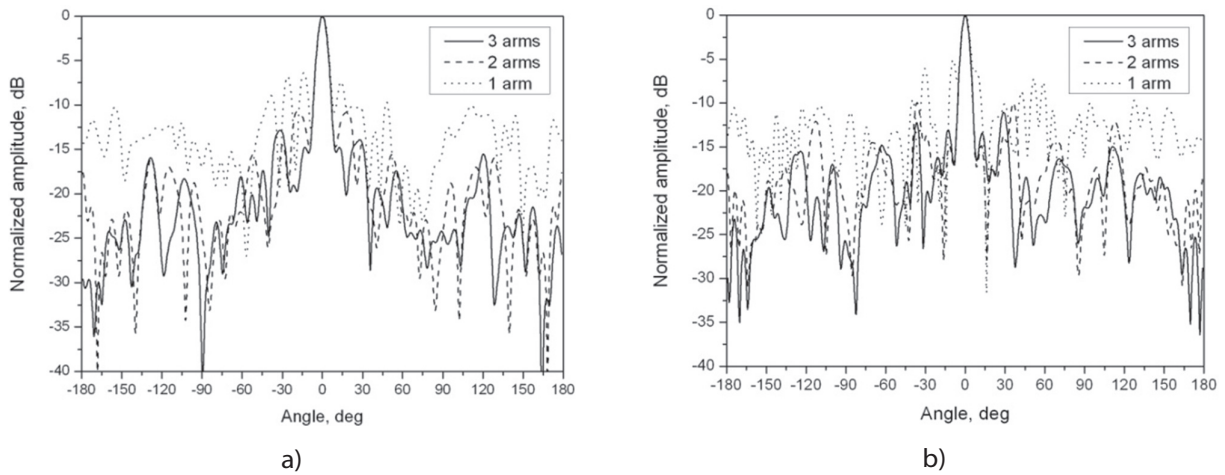**Fig. 13.** Normalized radiation pattern for a different number of antennas if a = 0.20
a) the E plane and b) the H plane.

If a = 0.20, the SLL decreases from -6.33 dB (a one-arm Archimedean spiral) to -12.83 dB (a three-arm Archimedean spiral) in the E-plane, and from -5.05 dB (a one-arm Archimedean spiral) to -11.06 dB (a three-arm Archimedean spiral) in the H-plane.
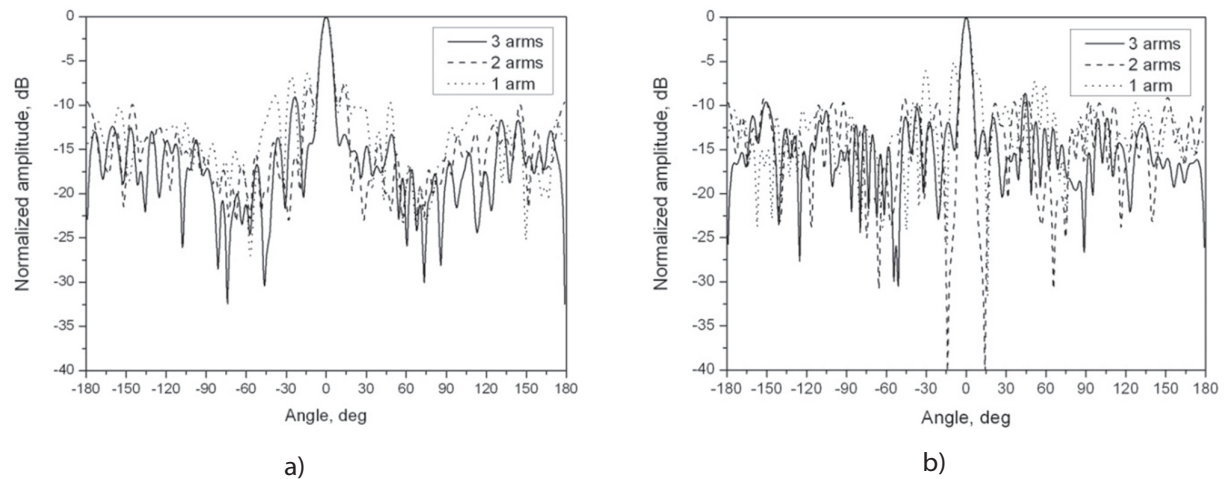

Fig. 14. Normalized radiation pattern for a different number of antennas if a = 0.25
a) the E plane and b) the H plane.

B) The MIN$_{SLL}$ and MAX$_{SLL}$ planes

Since the considered arrays do not possess a regular grid, we have to check how the radiation pattern looks like for other planes.
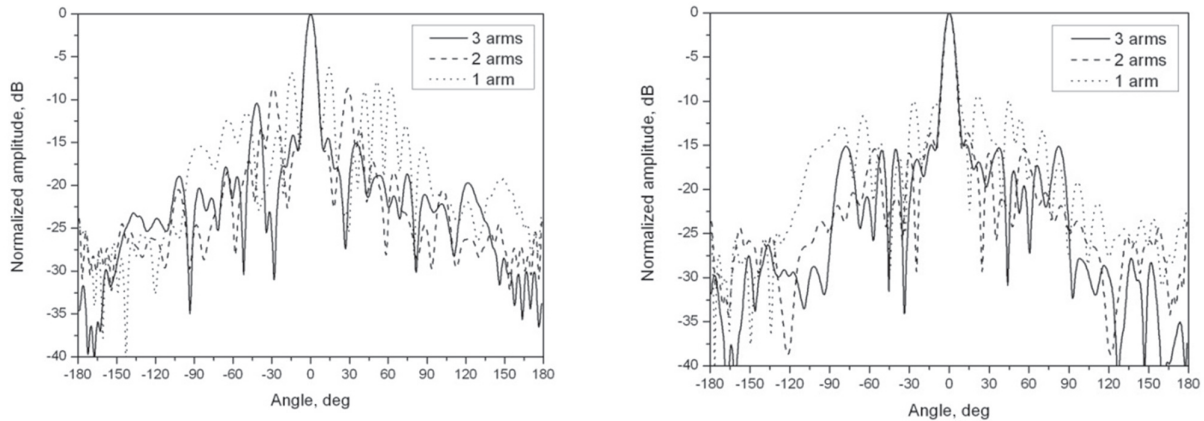

Fig. 15. Normalized radiation pattern for a different number of antennas if $a = 0.15$
a) the MIN$_{SLL}$ plane and b) the MAX$_{SLL}$ plane.

For these reasons we check side-lobe levels for all three antenna distributions in two more planes, i.e., the plane with the highest SLL and the plane with the lowest SLL. The planes considered (angle phi) are different for different distributions (Table 2).

Table 2.

	MIN$_{SLL}$		MAX$_{SLL}$	
	PHI, deg	SLL, dB	PHI, deg	SLL, dB
One arm	80.00	-6.25	162.00	-9.31
Two arms	146.00	-8.76	56.00	-13.57
Three arms	125.00	-10.50	14.00	-14.70

Results are presented in Figure 15 only for distributions with a=0.15.

An increase in the number of antennas has also improved the radiation pattern consequently (Figure 15). The SLL decreases from -6.25 dB (a one-arm Archimedean spiral) to -10.50 dB (a three-arm Archimedean spiral) in the MIN$_{SLL}$-plane. The SLL decreases from -9.31 dB (a one-arm Archimedean spiral) to -14.70 dB (a three-arm Archimedean spiral) in the MAX$_{SLL}$-plane.

Radiation patterns with a different direction of maximum radiation are not considered in this paper.

5. CONCLUSION

The presented numerical computations investigate the influence of three different Archimedean spiral distributions on the radiation pattern of spherical antenna arrays, i.e., one, two and three arms of Archimedean spiral distributions. All these conformal arrays differ from each other with respect to the elementary antenna number.

The method of analysis is based on the moment method where the elements of the moment method matrix are calculated in the spectral domain.

There were a few ways to influence the radiation pattern, but varying antenna density and changing the value of a (Equation (4)) were chosen.

All investigations lead to the same conclusions. It is obvious that a larger number of antenna elements in the appropriate array results in better radiation pattern characteristics. The main lobe of the diagram is narrower, and side lobe levels are decreased for a few dB.

As said before, a general mathematical notation for this kind of array is $\rho = a\varphi$. It was found out that parameter a has a considerable influence on the radiation pattern. By decreasing values from $a = 0.25$ to $a = 0.15$, side lobe levels are much better and could differentiate in 4 dB from the worst case (see Table 1).

The situation with pattern characteristics could be improved by applying array parameter optimization – as adopted in a few previous papers (e.g., [3] and [5]). This paper will not deal with optimization; these three types of configuration are compared only in regard to radiation pattern characteristics. Radiation pattern optimization and verification by comparison with measured results will be left for future work.

6. REFERENCES

[1] L. Marantis, E.D. Witte, P.V. Brennan, "Comparison of Various Spherical Antenna Array Element Distributions", Antennas and Propagation 2009, EuCAP 2009. 3rd European Conference, pp. 2980-2984, Berlin, Germany, March 2009.

[2] V. Mandrić, S. Rupčić, D. Žagar, "Optimization of the Spherical Antenna Arrays", Proceedings of EL-MAR 2012, pp. 287-292, Zadar, Croatia, September 2012.

[3] V. Mandrić, S. Rupčić, D. Pilski, "Experimental Results of Spherical Arrays of Circular Waveguide and

Microstrip Antennas", Proceedings of ELMAR 2011, pp. 345-351, Zadar, Croatia, September 2011.

[4] S. Rupčić, V. Mandrić, "Spiral Antenna Array Configurations on Spherical Surface", Applied Electromagnetics and Communications (ICECom), 21st International Conference, pp. 1-5, Dubrovnik, Croatia, October 2013.

[5] V. Mandric,"Radiation pattern optimization for antenna arrays on spherical surface", Doctoral dissertation, Faculty of Electrical Engineering, Josip Juraj Strossmayer University of Osijek, Osijek, Croatia, June 2012. (in Croatian)

[6] P.-S. Kildal, J. Sanford, "Analysis of conformal antennas by using spectral domain technique for curved structures", Proceedings of COST 245 – ESA Workshop on Active Antennas, pp. 17-26, Noordwijk, Netherlands, June 1996.

[7] Z. Sipus, P.-S. Kildal, R. Leijon, M. Johansson, "An algorithm for calculating Green's functions for planar, circular cylindrical and spherical multilayer substrates", Applied Computational Electromagnetics Society Journal, Vol. 13, No. 3, pp. 243-254, USA, November 1998.

[8] D. Dunham, "Hyperbolic Spirals and Spiral Patterns", Meeting Alhambra, ISAMA-BRIDGES Conference Proceedings, Granada, Spain, pp. 521-528, 2003.